Published in final edited form as:
Int J Cancer. 2011 October 1; 129(7): 1671–1677. doi:10.1002/ijc.26113.

Near infrared fluorescence-guided real-time endoscopic detection of peritoneal ovarian cancer nodules using intravenously injected indocyanine green

Nobuyuki Kosaka, **Makoto Mitsunaga**, **Michelle R. Longmire**, **Peter L Choyke**, and **Hisataka Kobayashi**
Molecular Imaging Program, Center for Cancer Research, National Cancer Institute, National Institutes of Health, Bethesda, Maryland 20892-1088, USA

Abstract

Near infrared fluoresce-guidance can be used for the detection of small cancer metastases and can aid in the endoscopic management of cancer. Indocyanine green (ICG) is an FDA-approved fluorescence agent. Through non-specific interactions with serum proteins, ICG achieves enhanced permeability and retention (EPR) effects. Yet, ICG demonstrates rapid clearance from the circulation. Therefore, ICG may be an ideal contrast agent for real-time fluorescence imaging of tumors. To evaluate the usefulness of real-time dual fluorescence and white light endoscopic optical imaging to detect tumor implants using the contrast agent ICG, fluorescence-guided laparoscopic procedures were performed in mouse models of peritoneally disseminated ovarian cancers. Animals were administered intravenous ICG or a control contrast agent, IR800-conjugated to albumin. The ability to detect small ovarian cancer implants was then compared. Using the dual view microendoscope, ICG clearly enabled visualization of peritoneal ovarian cancer metastatic nodules derived from SHIN3 and OVCAR5 cells at 6 and 24 h after injection with significantly higher tumor-to-background ratio than the control agent, (IR800-albumin $p<0.001$). In conclusion, ICG has the desirable properties of having both EPR effects and rapid clearance for the real-time endoscopic detection of tiny ovarian cancer peritoneal implants compared to a control macromolecular agent with theoretically better EPR effects but longer circulatory retention. Given that ICG is already FDA-approved and has a long track record of human use, this method could be easily translated to the clinic as a robust tool for fluorescence-guided endoscopic procedures for the management and treatment of cancer.

Keywords

cancer; endoscopy; near infrared; indocyanine green; surgery assistance

Correspondence to: Hisataka Kobayashi, M.D., Ph.D. Molecular Imaging Program, National Cancer Institute, NIH, Building 10, Room B3B69, MSC1088, Bethesda, MD 20892-1088. Phone: 301-451-4220; Fax: 301-402-3191; kobayash@mail.nih.gov.

Novelty and impact of this work is to be: In this article, we describe the use of indocyanine green (ICG) in detecting ovarian cancer. ICG is an FDA-approved fluorescence agent, which possesses unique pharmacokinetic characteristics that permit effective optical tumor imaging through enhanced permeability and retention effects (EPR), a phenomenon generally limited to much larger molecules. ICG demonstrates both macro- and micro-molecular behavior in circulation; through avid binding of serum proteins ICG achieves EPR effects typical of larger molecules yet retains rapid clearance from the circulation, like a small molecule. Therefore, ICG is a potentially powerful contrast agent for fluorescence-guided tumor detection of even tiny metastases. As shown herein, ICG demonstrated better ability for detecting small foci of peritoneally-disseminated metastatic ovarian cancer than a macromolecular fluorescent albumin with a white light/NIR fluorescence dual mode endoscope system. Since ICG is already FDA-approved as a contrast agent for clinical use, this method could be easily translated to the clinic as a tool for fluorescence-guided endoscopic cancer detection and surgery.

Introduction

Fluorescence imaging has proven to be a useful tool in biological research with a long record of success for *in vitro* cellular imaging. Fluorescence imaging has recently been found to be useful for *in vivo* preclinical [1, 2] and clinical applications as well [3–5]. Optical imaging has numerous advantages: 1) high sensitivity, 2) high frame rate, 3) relatively low cost, 4) portability, 5) lack of radiation exposure, and 6) the ability to multiplex several colors at once [4]. Real-time imaging, which is defined as acquiring serial images at frame rates of more than several frames per second, makes it possible to use imaging during surgery, endoscopy or interventional procedures [6]. For these reasons, real-time optical imaging is an attractive method for early cancer detection, lymphatic imaging as well as for image-guided interventions [3, 5].

Indocyanin green (ICG) and fluorescein are the only two fluorescent contrast agents approved by the Food and Drug administration (FDA) in the United States for use in retinal angiography and have been in human use for decades with an excellent safety profile. ICG, which emits near infrared fluorescence, has been used as well in hepatic function testing [7]. In circulation, ICG shows reversible binding to serum proteins. Because it has both lipophilic and hydrophilic properties, ICG is 98% protein-bound *in vivo*. Although it was previously thought to bind primarily to serum albumin [8], ICG molecules have also been shown to bind to serum globulins such as alpha1-lipoprotein (a high density lipoprotein) [9]. Unlike the unbound molecule, highly protein bound ICG behaves like a macromolecule in circulation. As a result, successful lymphatic imaging, including lymphangiography in extremities with lymphedema [10] and sentinel node detection [3, 11–15], can be accomplished using ICG as a contrast agent.

It is well known that macromolecules often demonstrate enhanced permeability and retention (EPR) effects within the tumor tissue, secondary to immature and leaky tumor vessels that result from tumor-induced angiogenesis [16, 17]. EPR effects have been utilized to improve drug delivery to cancers [16]. However, the usefulness of EPR effects in tumor imaging has been somewhat limited as the phenomenon is observed with macromolecules, which have long circulatory retention times. Therefore, in the case of macromolecular contrast agents, long circulation times result in high background signal, reducing the tumor-to-background signal intensity ratio (TBR) [18]. Although ICG is a small molecule, it behaves like a large molecule after binding to serum proteins; yet, demonstrates relatively rapid clearance from the blood circulation with normal hepatic function. Therefore, we hypothesized that ICG would provide better tumor imaging at earlier time points than typical macromolecules, in this case, a covalently bound macromolecular imaging agent. In this study, we compare ICG, with its relatively weak protein binding, to a covalently bound albumin-based IR800 imaging agent, for the detection of ovarian cancer implants using a micro-endoscope equipped with capabilities for fluorescence imaging.

Materials and Methods

Reagents

Indocyanine green (ICG) and human serum albumin (HSA) were purchased from Sigma-Aldrich (St. Louis, MO). The NHS ester of IRDye 800CW (IR800) was purchased from LI-COR (Lincoln, NE).

Synthesis of HSA-IR800

HSA (6 nmol) was incubated with IR800 (60 nmol) in 0.1 M Na_2HPO_4 (pH 8.5) at room temperature for 15 min. Each mixture was purified with a Sephadex G25 column (PD-10; GE Healthcare, Piscataway, NJ). The protein concentration was determined by measuring

the absorption at 280 nm with a UV-Vis system (8453 Value UV-visible Value System; Agilent Technologies, Santa Clara, CA). The concentration of IR800 was measured by absorption with the UV-Vis system to confirm the number of fluorophore molecules conjugated to HSA. The number of fluorophore molecules per all HSA conjugates was ~2.0.

Cell line and cell culture

The established human ovarian cancer cell lines, SHIN3 [19] and OVCAR5 [20] were used for generating intraperitoneal disseminated tumors. The cell lines were grown in RPMI 1640 medium (Invitrogen Corporation, Carlsbad, CA) containing 10% fetal bovine serum (FBS) (Invitrogen Co.), 0.03% L-glutamine at 37 °C, 100 units/mL penicillin, and 100 μg/mL streptomycin in 5% CO_2.

Tumor model

All procedures were approved by the National Cancer Institute Animal Care and Use Committee. The intraperitoneal tumor implants were established by intraperitoneal injection of 2×10^6 either SHIN3 or OVCAR5 cells suspended in 200 μL of PBS in female nude mice (National Cancer Institute Animal Production Facility, Frederick, MD). Experiments with tumor bearing mice were performed 15–20 days after inoculation.

In vivo fluorescence imaging of peritoneal disseminated tumor nodules

In vivo real-time fluorescence endoscopic study was performed with a clinical endoscopic system (EVIS ExERA-II CLV-180, Olympus Corp., Tokyo, Japan) equipped with an in-house fluorescence system. Excitation and emission filters were 600±200 nm band-pass and 842.5±17.5 nm band-pass, respectively. SHIN3 or OVCAR5 tumor-bearing mice (n=4–5, each) were anesthetized by intravenous injection of 1.15 mg sodium pentobarbital (Nembutal Sodium Solution, Ovation Pharmaceuticals Inc., Deerfield, IL). The endoscope was inserted into the abdominal cavity thorough a small abdominal incision, and then the abdominal cavity was inflated with air. After obtaining control (un-enhanced) fluorescence images of peritoneal disseminated nodules, either 100 μL of 1mM ICG diluted with PBS or 100 μg of HSA-IR800 in 100 μL PBS was intravenously injected through the tail vein and real-time fluorescence imaging was recorded for the first 10min and then at 1 hr. Other sets of SHIN3 or OVCAR-bearing mice (n=4–5, each) were intravenously injected with either 100 μL of 1mM ICG diluted with PBS or 100 μg of HSA-IR800 in 100 μL PBS, and *in vivo* real-time fluorescence endoscopic studies were performed with the same procedures as above but at 6 h and 24 h.

After the fluorescence endoscopic study, all mice were sacrificed with carbon dioxide, and the abdominal cavities were exposed, and subjected to whole body spectral fluorescence imaging. Spectral fluorescence images were obtained using the Maestro *In-Vivo* imaging system (CRi, Inc., Woburn, MA). The near-infrared filter setting (excitation filter: 735±50 nm band-pass and emission filter: 800 long-pass) was used. The tunable filter was automatically stepped in 10 nm increments from 650 to 950 nm, while the camera sequentially captured images at each wavelength interval. The spectral fluorescence images consisting of autofluorescence and ICG or IR800 spectra were unmixed for visual assessments using commercial software (Maestro software, CRi). After all imaging procedures, 4–5 tumor nodules of each mouse were harvested and subjected to histological validation with hematoxylin-eosin staining.

Semi-quantitative image analysis of fluorescence endoscopic images

Recorded endoscopic videos were captured and converted to TIFF format still images for semi-quantitative image analysis. Regions of interest (ROIs) were drawn over the tumor

nodules based on white-light images. Three small circular ROIs were also placed over images of the adjacent background parietal peritoneum, and fluorescence intensity (arbitrary unit: a.u.) of tumor nodules and backgrounds (average of three ROIs) were measured with Image J software (http://rsbweb.nih.gov/ij/). Finally, tumor-to-background ratios (TBR) were calculated for each tumor nodule.

Statistical analysis

Statistical analysis was performed using a statistics program (GraphPad Instat, version 3.06, GraphPad Software, La Jolla, CA) on a Windows computer. A one-way analysis of variance (ANOVA) with post test (Kruskal-Wallis test with Dunn's multiple comparisons test) was used to compare the means of TBRs at 1, 6, and 24 h in each group. Values of $p < 0.05$ were considered statistically significant.

Results

Immediately after intravenous injection of ICG solution, SHIN3 disseminated tumor nodules and parietal peritoneal vessels were optically enhanced, as shown in Figure 1 and supplementary video 1. However, this tumor enhancement gradually decreased with time, whereas background signal increased, resulting in unclear tumor depictions on fluorescence images at 1 h after injection (Fig. 1 and supplementary video 2). After another 5 h (6 h after injection), background signal was diminished and then tumor nodules were clearly depicted with high tumor-to-background ratios (Fig. 1 and supplementary video 3). At 24 h after injection, tumor nodules were still clearly depicted with low background signals, but the camera gain had to be increased 45% due to lower overalls signal (Fig. 1). Similar findings were present in OVCAR 5 tumor-bearing mice, although tumor enhancement was slightly weaker than that in SHIN3 tumors (Fig. 1 and supplementary video 4).

In contrast to these findings with ICG, SHIN3 mice receiving HSA-IR800 was less effective. Within the first 5 minutes post injection, optical enhancement of the tumor and peritoneal vessels were observed as with ICG, however, unlike ICG, these vascular enhancements persisted even 1 h after injection due to slow clearance of HSA-IR800 (Fig. 1). Furthermore, in contrast to ICG, HSA-IR800 showed very high background signal even at 6 h and 24 h after injection, thus hampering efforts to visualize disseminated tumor nodules (Fig. 1)

These subjective results were supported by semi-quantitative analysis of fluorescence endoscopic images. A total of 542 disseminated nodules were evaluated (SHIN3-ICG group: 41 at 1 h, 55 at 6 h, and 49 at 24 h. OVCAR5-ICG group: 58 at 1 h, 85 at 6 h, and 80 at 24 h. SHIN3-HSA-IR800 group: 49 at 1 h, 71 at 6 h, and 54 at 24 h). Mean and standard deviation (SD) of each group were summarized in Figure 2. In the SHIN3-ICG group, TBRs at 6 h (mean ± SD: 1.71 ± 0.20) and at 24 h (1.73 ± 0.23) were statistically higher than that at 1 h (1.17 ± 0.17). TBRs between 6 h and 24 h did not statistically differ. Furthermore, in the OVCAR5-ICG group TBRs at 6 h (1.43 ± 0.17) and 24 h (1.47 ±0.20) were also statistically higher than those at 1 h (1.24 ± 0.17). In contrast to the ICG group, the TBRs in SHIN3-HSA-IR800 group did not show statistical differences among the time points (1.19 ± 0.19 at 1 h, 1.20 ± 0.17 at 6 h, and 1.22 ± 0.14 at 24 h, respectively).

Whole body spectral fluorescence imaging clearly demonstrated differences in pharmacokinetics between ICG and HSA-IR800 (Fig. 3). At 1 h after injection, ICG accumulated in the liver and was excreted into the small intestine through biliary clearance. This liver uptake decreased with time, while bowel (feces) uptake increased at 6 h. Twenty-four h later, ICG containing feces were cleared from the bowel, and the tumor nodules were clearly depicted with low background signal. In contrast to ICG, the mice treated with HSA-

IR800 showed high body background at all time points due to slow clearance from circulation.

All 32 and 29 fluorescent nodules of 1–2 mm in size sampled from the mouse peritoneum of ICG-injected, SHIN3 or OVCAR5 peritoneal implant bearing mice, respectively, were confirmed as cancer nodules by histological analysis with hematoxylin-eosin staining (Fig. 4). However, 40 non-fluorescent adjacent tissue samples (20 samples each from ICG-injected SHIN3 or OVCAR5 peritoneal implant bearing mice) did not contain cancer tissue. Therefore, fluorescent nodules of 1–2 mm in size, which had similar sizes to tumors observed under *in vivo* fluorescence endoscopy, were visualized with ICG injection of 100% sensitivity and 100% specificity.

Discussion

In this study, we compared the efficacy of ICG, an FDA-approved fluorophore, to a control macromolecular fluorescence agent, IR800-conjugated albumin, in their ability to detect ovarian peritoneal metastases using laparoscopic optical imaging. NIR fluorescence-guided laparoscopy was performed on mice treated with either intravenously administered ICG or IR800-conjugated albumin. IR800-conjugated albumin was chosen as a control because of its optimal EPR effects. ICG-albumin was not chosen as a control, since covalently binding ICG can change its optical characteristics leading to quenching of the fluorophore [21]. In addition, although IR800 did not show noticeable non-specific binding to albumin, it is not possible to perfectly separate non-specific albumin-binding fraction of free ICG from covalently bound ICG with the gel-filtration. Therefore, IR800-albumin was felt to be a better control than ICG-albumin, when compared with free ICG, which showed “partial” EPR effects and rapid clearance from the circulation.

As shown in the videos, near infrared (NIR) endoscopy has the advantage of real time dual imaging of white light and NIR fluorescence. Since NIR fluorophores can be excited with broad visible range light, white light imaging is not compromised. Using an optical splitter, consisting of a dichroic mirror, simultaneous display of white light and NIR fluorescence images in real time was achieved. Therefore, interventional procedures under the endoscope can be performed easily.

As shown in *in vivo* imaging, ICG was hepatically cleared and excreted through the bile. As a result, fluorescence signal in the liver and intestine was high within 6 h. However, tiny peritoneal implants derived from both ovarian cancer cell lines were clearly detected at 6 h after injection of ICG and became clearer at 24 h after injection. In contrast, IR800-albumin showed higher fluorescence signal in blood vessels than in the tumor implants even at 24 h after injection. Both ICG and IR800-albumin showed EPR effects, however, the rapid clearance of ICG, resulted in a better TBR at more delayed time points. The difference in circulatory half-lives is attributed to the relatively weak fluorophore-protein interactions of ICG compared to the covalently bound IR800-albumin.

Unlike ICG, none of the existing imaging agents that have been reported in the literature are already FDA approved. ICG has a history of over 50 years of safe use in humans. Therefore, in order to translate research agents into the clinic, it will be necessary to file a investigative new drug (IND) application, which will require extensive toxicity testing and good manufactured product (GMP) grade manufacturer, only achievable after a substantial monetary investment. Additionally, several of the new optical imaging agents are targeted to specific cell surface markers such as HER1 [22], folate receptor [23], or lectin families [24], which may or may not be expressed on all cancer cells. A disadvantage of ICG compared to targeted agents is that some of these reagents could be activatable upon binding to the target

molecules, yielding very high target to background ratios [24, 25]. Such agents could demonstrate superior sensitivity and specificity to ICG, and therefore merit consideration. However, none of these agents is as easy to apply in humans as ICG. ICG has already been approved for the clinical use for other applications such as retinal angiography and hepatic clearance studies. Therefore, the method described herein is ready for clinical translation involving fluorescence-guided laparoscopic detection of ovarian cancer with IRB approval for off-label use. A wide time window for successful imaging, 6 to 24 h after injection, facilitates the practical clinical application of this method. Thus, ICG could be injected pre-operatively but would retain efficacy throughout the procedure. We believe, this method could have broad application in other accessible cancers with endoscopes such as colon cancer, mesotheliomas in the pleura and bladder cancers in the bladder.

Supplementary Material

Refer to Web version on PubMed Central for supplementary material.

Acknowledgments

This research was supported by the Intramural Research Program of the National Institutes of Health, National Cancer Institute, Center for Cancer Research.

References

1. Hoffman RM. The multiple uses of fluorescent proteins to visualize cancer in vivo. Nat Rev Cancer. 2005; 5:796–806. [PubMed: 16195751]
2. Weissleder R. A clearer vision for in vivo imaging. Nat Biotechnol. 2001; 19:316–7. [PubMed: 11283581]
3. Kitai T, Inomoto T, Miwa M, Shikayama T. Fluorescence navigation with indocyanine green for detecting sentinel lymph nodes in breast cancer. Breast Cancer. 2005; 12:211–5. [PubMed: 16110291]
4. Kosaka N, Ogawa M, Choyke PL, Kobayashi H. Clinical implications of near-infrared fluorescence imaging in cancer. Future Oncol. 2009; 5:1501–11. [PubMed: 19903075]
5. Ntziachristos V, Yodh AG, Schnall M, Chance B. Concurrent MRI and diffuse optical tomography of breast after indocyanine green enhancement. Proc Natl Acad Sci U S A. 2000; 97:2767–72. [PubMed: 10706610]
6. Kosaka N, McCann TE, Mitsunaga M, Choyke PL, Kobayashi H. Real-time optical imaging using quantum dot and related nanocrystals. Nanomedicine (Lond). 2010; 5:765–76. [PubMed: 20662647]
7. Alford R, Simpson HM, Duberman J, Hill GC, Ogawa M, Regino C, Kobayashi H, Choyke PL. Toxicity of organic fluorophores used in molecular imaging: literature review. Mol Imaging. 2009; 8:341–54. [PubMed: 20003892]
8. Cherrick GR, Stein SW, Leevy CM, Davidson CS. Indocyanine green: observations on its physical properties, plasma decay, and hepatic extraction. J Clin Invest. 1960; 39:592–600. [PubMed: 13809697]
9. Baker KJ. Binding of sulfobromophthalein (BSP) sodium and indocyanine green (ICG) by plasma alpha-1 lipoproteins. Proc Soc Exp Biol Med. 1966; 122:957–63. [PubMed: 5918158]
10. Sevick-Muraca EM, Sharma R, Rasmussen JC, Marshall MV, Wendt JA, Pham HQ, Bonefas E, Houston JP, Sampath L, Adams KE, Blanchard DK, Fisher RE, et al. Imaging of lymph flow in breast cancer patients after microdose administration of a near-infrared fluorophore: feasibility study. Radiology. 2008; 246:734–41. [PubMed: 18223125]
11. Miyashiro I, Miyoshi N, Hiratsuka M, Kishi K, Yamada T, Ohue M, Ohigashi H, Yano M, Ishikawa O, Imaoka S. Detection of sentinel node in gastric cancer surgery by indocyanine green fluorescence imaging: comparison with infrared imaging. Ann Surg Oncol. 2008; 15:1640–3. [PubMed: 18379850]

12. Motomura K, Inaji H, Komoike Y, Kasugai T, Noguchi S, Koyama H. Sentinel node biopsy guided by indocyanine green dye in breast cancer patients. Jpn J Clin Oncol. 1999; 29:604–7. [PubMed: 10721942]

13. Nimura H, Narimiya N, Mitsumori N, Yamazaki Y, Yanaga K, Urashima M. Infrared ray electronic endoscopy combined with indocyanine green injection for detection of sentinel nodes of patients with gastric cancer. Br J Surg. 2004; 91:575–9. [PubMed: 15122608]

14. Tanaka R, Nakashima K, Fujimoto W. Sentinel lymph node detection in skin cancer using fluorescence navigation with indocyanine green. J Dermatol. 2009; 36:468–70. [PubMed: 19691754]

15. Yamashita S, Tokuishi K, Anami K, Miyawaki M, Moroga T, Kamei M, Suehiro S, Ono K, Takeno S, Chujo M, Yamamoto S, Kawahara K. Video-assisted thoracoscopic indocyanine green fluorescence imaging system shows sentinel lymph nodes in non-small-cell lung cancer. J Thorac Cardiovasc Surg. 2011; 141:141–4. [PubMed: 20392454]

16. Maeda H, Matsumura Y. EPR effect based drug design and clinical outlook for enhanced cancer chemotherapy. Adv Drug Deliv Rev. 2010

17. Matsumura Y, Maeda H. A new concept for macromolecular therapeutics in cancer chemotherapy: mechanism of tumoritropic accumulation of proteins and the antitumor agent smancs. Cancer Res. 1986; 46:6387–92. [PubMed: 2946403]

18. Kobayashi H, Ogawa M, Alford R, Choyke PL, Urano Y. New strategies for fluorescent probe design in medical diagnostic imaging. Chem Rev. 2010; 110:2620–40. [PubMed: 20000749]

19. Imai S, Kiyozuka Y, Maeda H, Noda T, Hosick HL. Establishment and characterization of a human ovarian serous cystadenocarcinoma cell line that produces the tumor markers CA-125 and tissue polypeptide antigen. Oncology. 1990; 47:177–84. [PubMed: 2314830]

20. Hamilton TC, Young RC, Ozols RF. Experimental model systems of ovarian cancer: applications to the design and evaluation of new treatment approaches. Semin Oncol. 1984; 11:285–98. [PubMed: 6385258]

21. Ogawa M, Kosaka N, Choyke PL, Kobayashi H. In vivo molecular imaging of cancer with a quenching near-infrared fluorescent probe using conjugates of monoclonal antibodies and indocyanine green. Cancer Res. 2009; 69:1268–72. [PubMed: 19176373]

22. Hama Y, Urano Y, Koyama Y, Choyke PL, Kobayashi H. Activatable fluorescent molecular imaging of peritoneal metastases following pretargeting with a biotinylated monoclonal antibody. Cancer Res. 2007; 67:3809–17. [PubMed: 17440095]

23. Kalli KR, Oberg AL, Keeney GL, Christianson TJ, Low PS, Knutson KL, Hartmann LC. Folate receptor alpha as a tumor target in epithelial ovarian cancer. Gynecol Oncol. 2008; 108:619–26. [PubMed: 18222534]

24. Hama Y, Urano Y, Koyama Y, Kamiya M, Bernardo M, Paik RS, Shin IS, Paik CH, Choyke PL, Kobayashi H. A target cell-specific activatable fluorescence probe for in vivo molecular imaging of cancer based on a self-quenched avidin-rhodamine conjugate. Cancer Res. 2007; 67:2791–9. [PubMed: 17363601]

25. Hama Y, Urano Y, Koyama Y, Gunn AJ, Choyke PL, Kobayashi H. A self-quenched galactosamine-serum albumin-rhodamineX conjugate: a “smart” fluorescent molecular imaging probe synthesized with clinically applicable material for detecting peritoneal ovarian cancer metastases. Clin Cancer Res. 2007; 13:6335–43. [PubMed: 17975145]

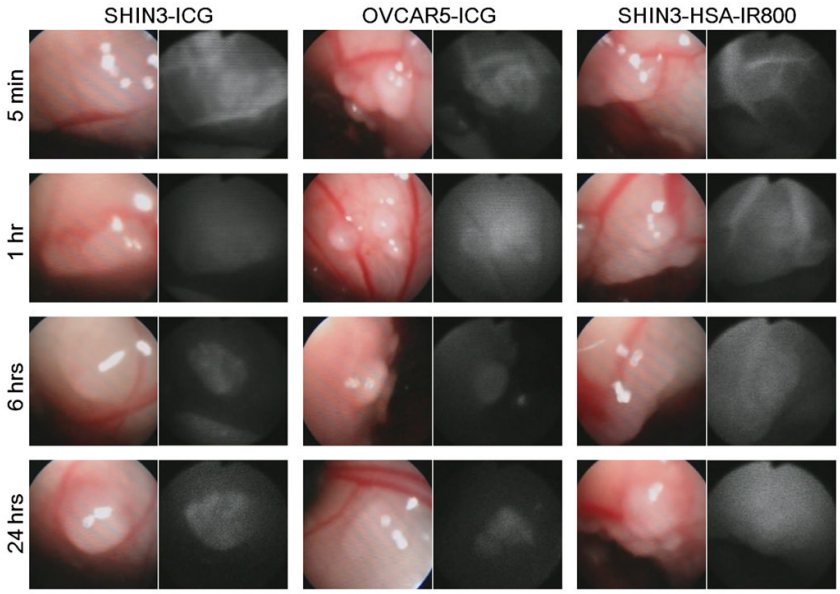

Fig. 1. ICG clearly depicts disseminated peritoneal ovarian cancer nodules

In vivo real-time fluorescence endoscopic images of each group at each time point are shown. Disseminated tumor nodules as small as 0.3 mm in diameter are clearly depicted with ICG at 6 and 24 h after injection.

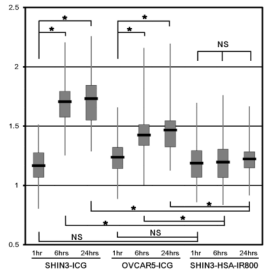

Fig. 2. Tumor-to-background ratio improves after ICG injection

Semi-quantitative analysis of fluorescence endoscopic images is shown. Vertical axis is tumor-to-background ratio (TBR). TBRs at 6 and 24 h in ICG groups are statistically higher than those at 1 h or those in HSA-IR800 group at the same time points (*$p<0.001$).

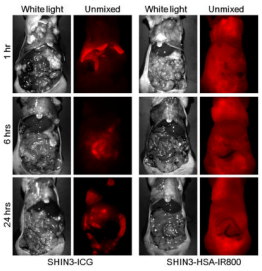

Fig. 3. ICG is retained in tumor and cleared from the background into the bile

Whole body spectral fluorescence images of SHIN3 tumor-bearing mice with either ICG or HSA-IR800 injections. The difference of pharmacokinetics between ICG and HSA-IR800 is clearly demonstrated.

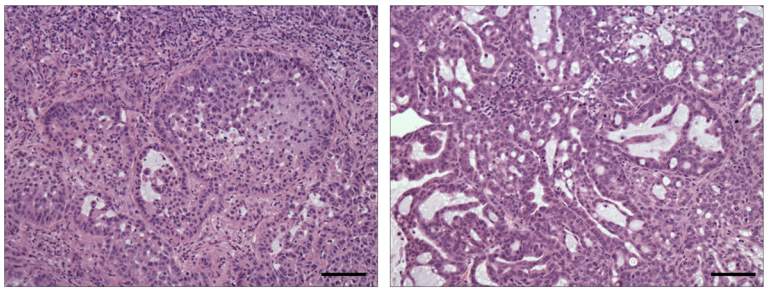

Fig. 4. All fluorescent nodules were validated as cancer metastasis

Hematoxylin-eosin staining of disseminated tumor nodules derived from SHIN3 and OVCAR5. OVCAR5 tumor contains more mucinous and less cellular component than SHIN3, resulting in less fluorescent signal.

Int J Cancer. Author manuscript; available in PMC 2012 October 1.

Table 1

Summary of tumor-to-background ratios (TBRs) of each group.

		n	Mean	Median	SD
SHIN3-ICG	**1 h**	41	1.17	1.16	0.17
	6 h	55	1.71	1.71	0.20
	24 h	49	1.73	1.76	0.23
OVCAR5-ICG	**1 h**	58	1.24	1.22	0.17
	6 h	85	1.43	1.39	0.17
	24 h	80	1.47	1.46	0.20
SHIN3-HSA-IR800	**1 h**	49	1.19	1.20	0.19
	6 h	71	1.20	1.21	0.17
	24 h	54	1.22	1.23	0.14

n: Number of tumor nodules. SD: Standard deviation.